Study of Forecasting Renewable Energies in Smart Grids Using Linear predictive filters and Neural Networks

Anvari-Moghaddam, Amjad; Seifi, Alireza

Published in:
IET Renewable Power Generation

Publication date:
2011

Techset Composition Ltd, Salisbury
Doc: H:/lee/RPG/Articles/Pagination/RPG20100104.3d

www.ietdl.org

Published in IET Renewable Power Generation
Received on 21st June 2010
Revised on 23rd April 2011
doi: 10.1049/iet-rpg.2010.0104

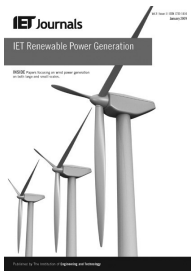

ISSN 1752-1416

Study of forecasting renewable energies in smart grids using linear predictive filters and neural networks

A. Anvari Moghaddam A.R. Seifi

Department of Power and Control, School of Electrical and Computer Engineering, Shiraz University, Engineering Faculty No. 1, Zand St, Shiraz, Iran
E-mail: seifi@shirazu.ac.ir

Abstract: Accurate forecasting of renewable energies such as wind and solar has become one of the most important issues in developing smart grids. Therefore introducing suitable means of weather forecasting with acceptable precision becomes a necessary task in today's changing power world. In this work, an intelligent way for hourly estimation of both wind speed and solar radiation in a typical smart grid has been proposed and its superior performance is compared to those of conventional methods and neural networks (NNs). The methodology is based on linear predictive coding and digital image processing principles using two dimensional (2-D) finite impulse response filters. Meteorological data have been collected during the period 1 January 2009 to 31 December 2009 from Casella automatic weather station (AWS) at Plymouth, UK. Numerical results indicate that a considerable improvement in forecasting process is achieved with 2-D predictive filtering compared to the conventional approaches.

1 Introduction

The ability to better integrate renewable energies is one of the driving factors in some smart grid installations. With low incorporation of renewable energies the total effect on grid operations is confined, but as the penetration of such resources increases, their mutual effects increase too. Nevertheless, exploitation of renewable energy sources may be problematic because of their variable and intermittent nature [1, 2] so accurate forecasting of such energy resources is regarded as a key component of a typical smart grid [3, 4].

Up until now, there have been many various models for predicting renewable energies, mostly based on physical methods or conventional statistical ones. For example, Muneer and co-workers [5, 6] developed a meteorological radiation model and cloud cover radiation model in the case of solar radiation forecasting. All the mathematical models [7, 8] applying radiation theories and local meteorological data as well as some empirical parameters influence solar irradiation. In the same way, many authors apply variety of models for wind speed forecasting such as recursive least squares regression or autoregressive integrated moving average methods that provide satisfactory prediction on the basis of observed time-series data and their correlations [9–11]. Recently, artificial neural networks (ANNs) with their inherent capability for non-linear functionality and accurate mapping are applied for prediction objectives to a great extent. Furthermore, the combination of NNs with other techniques such as fuzzy rules and wavelet transformations become the area of interest for most of researchers [12, 13].

In this study, we focus on an intelligent method of hourly forecasting for wind speed and solar radiation in a typical smart grid in order to assess the maximum power generation from these resources. The idea behind the work is different from those mentioned earlier and it is mainly established on interpretation of meteorological data in a two dimensional (2-D) visual model as will be described in the next section. Although such an idea and 2-D rendering of a time-series signals like solar radiation data was initially introduced by Hocaoğlu *et al.* in [14] using a limited number of prediction methods and later was improved by themselves, but the application of the idea is something new in the field of renewable energies particularly in wind speed forecasting. During the work, first a working definition is presented about linear predictive coding (LPC) and image filtering concepts, then through an illustrative study the efficiency of the purposed estimator is tested and compared to those of conventional methods and NNs. Simulation results indicate that 2-D predictive filters not only result in a more accurate estimation of hourly wind speed and solar radiation, but also enable better interpretation of meteorological data through different time horizons. Moreover, since the 2-D modelling is fed by actual and observed climatic data which include both meteorological changes and atmospheric effects such as temperature and cloud cover, provides more reliable information for operators. The meteorological data used in the work are collected during the period 1 January 2009–31 December 2009 from Casella automatic weather station (AWS) at Plymouth, UK. The weather station is located on the roof of the Fitzroy building, which is approximately 50 m above MSL and 15 m above ground level. The solarimeter is a highly sensitive pyranometer and measures the intensity of the total solar radiation received at the

Earth's surface. When connected to the AWS, two measurements are acquired. Firstly, the basic 1 min spot sample is used to add to the total solar radiation (TSR) statistical values. The second is a pseudo-sensor, which is allocated its own channel and records 'Sunshine Hours'. This channel has a resolution of 1 min and will over a report period indicate the number of minutes that the solar radiation has exceeded a pre-set value. The current threshold for the definition 'sunshine' as opposed to 'daylight' is 210 W/m^2. The anemometer is based on a three-cup rotor, with an accuracy of $\pm 1\%$ over 3 m/s. Starting velocity is 0.4 m/s and the maximum designed wind speed is 75 m/s.

2 Smart rendering meteorological data in a 2-D visual model

Classification of meteorological data in an image-like model indicates the smart idea of this paper and it is presented here to obtain better insight about LPC and 2-D digital filtering concepts. To begin the procedure first the whole recorded meteorological information must be arranged in a 2-D array as given in (1). In the resultant matrices, rows represent the number of days in a year and columns show different hours in a given day and each element inside the matrices represents solar radiation or wind speed value at a given hour of a particular day in the year.

$$R_{\text{Solar-Radiation}} = \begin{bmatrix} r_{1,1} & \cdots & r_{1,24} \\ \vdots & r_{i,j} & \vdots \\ r_{365,1} & \cdots & r_{365,24} \end{bmatrix}$$

$$V_{\text{Wind-Speed}} = \begin{bmatrix} v_{1,1} & \cdots & v_{1,24} \\ \vdots & v_{i,j} & \vdots \\ v_{365,1} & \cdots & v_{365,24} \end{bmatrix}$$

$r_{i,j}$, $v_{i,j}$ = solar radiation and wind speed at jth hour of ith day, respectively

$$i_{(\text{days})} = 1, 2, \ldots, 365$$
$$j_{(\text{hours})} = 1, 2, \ldots, 24 \quad (1)$$

For better understanding of hourly solar radiation and wind speed data two different plots are presented below.

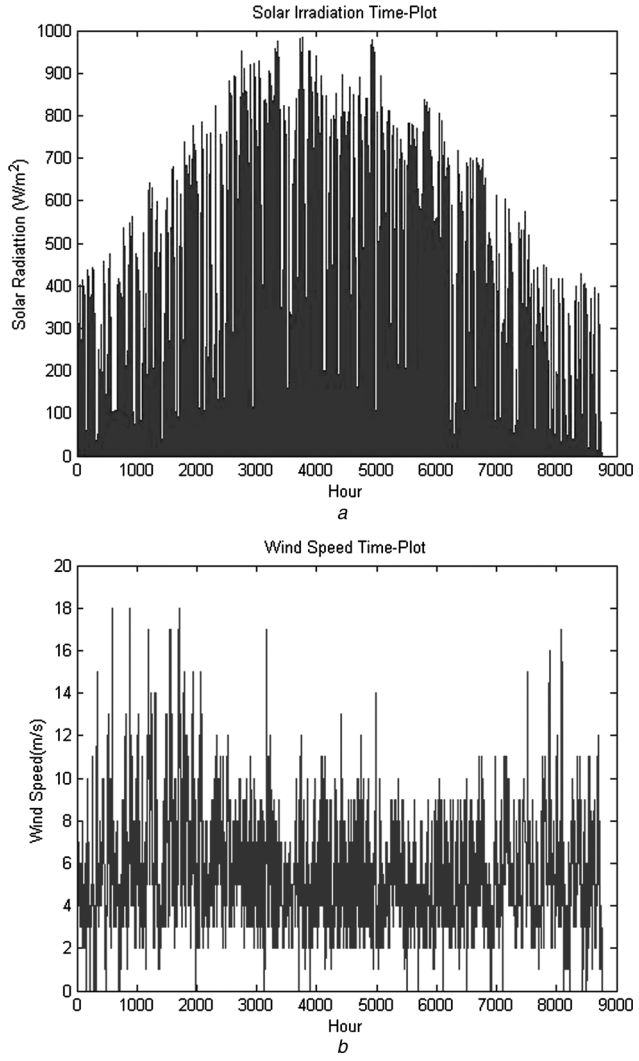

Fig. 1 *Time plot of meteorological data (1-D representation)*
a Hourly solar radiation
b Hourly wind speed

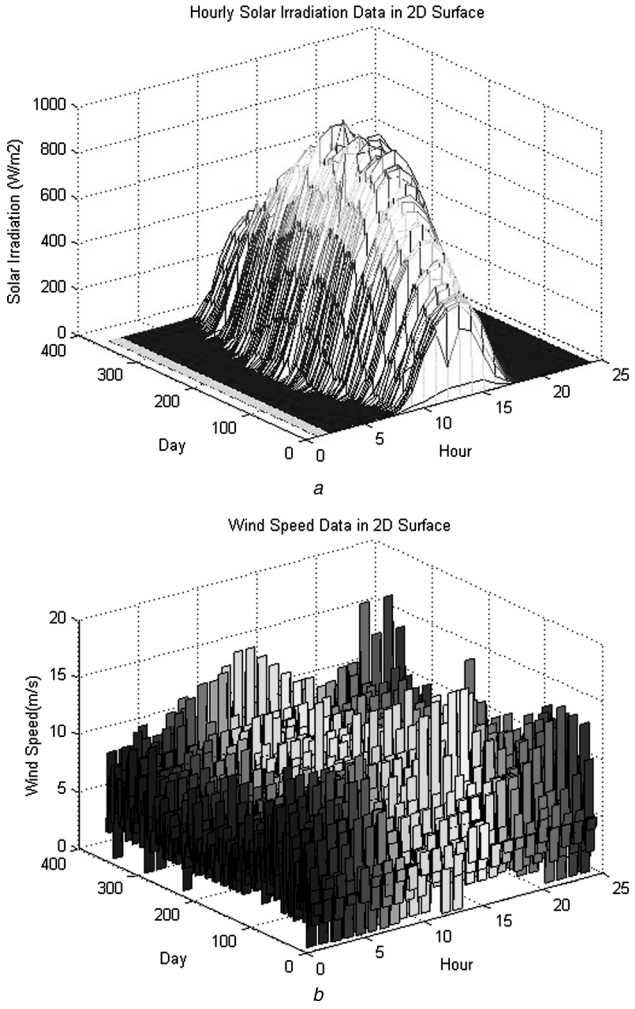

Fig. 2 *Surface plot of meteorological data (2-D representation)*
a Solar radiation
b Wind speed

doi: 10.1049/iet-rpg.2010.0104

First 1-D representation or time plot of climatic data (Figs. 1*a* and *b*) and second the 2-D representation or surface plot of mentioned information (Figs. 2*a* and *b*).

Two remarkable points can be observed from previous figures. First the periodical behaviour of solar radiation and the stochastic nature of wind speed is obvious from both 1-D and 2-D representations, but in the former it is troublesome to make distinction between irradiation and wind speed through different days and hours, whereas this interpretation is feasible in the latter. Now to make the image-like models complete, the surface models shown in Figs. 2*a* and *b* must be converted into grey-scale image as shown in Figs. 3*a* and *b*. In this image corresponding pixels represented by different grey values that range from white to black reveal hourly solar radiation and wind speed information in a smart form and this kind of indexed sequential access method guides us to a distinctive estimation approach via both LPC and 2-D image processing using expert finite impulse response (FIR) filters as will be explained later.

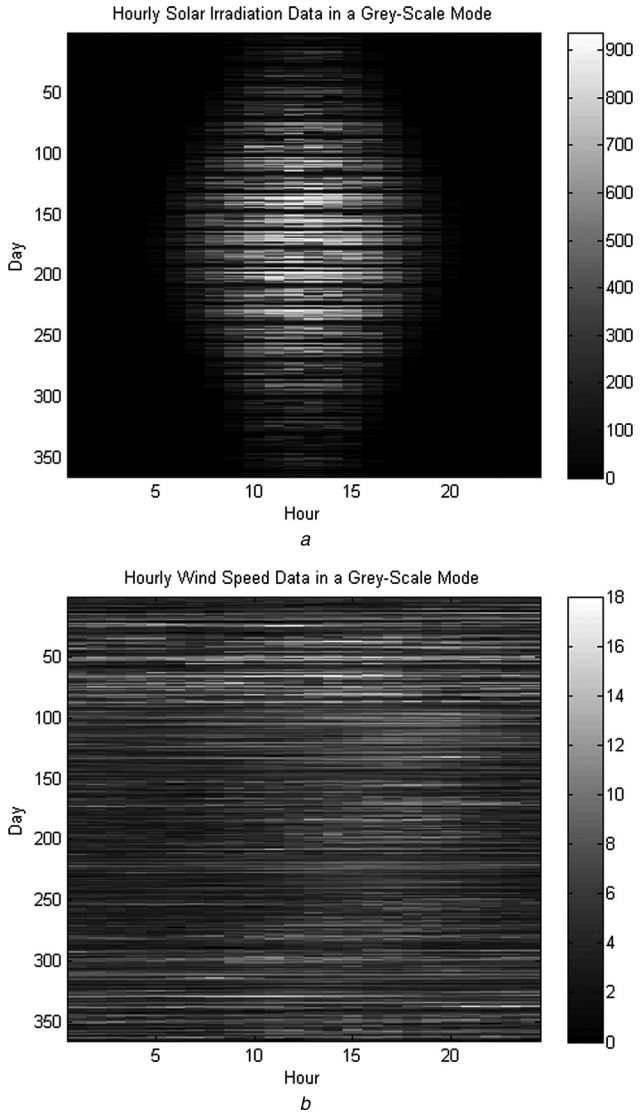

Fig. 3 *Rendering meteorological data in a grey-scale-image model*

a Solar radiation
b Wind speed

3 Fundamentals of predictive image filtering

Predictive filtering in the field of image processing is defined as a particular operation in which the scalar value of any given pixel inside the image range can be calculated by applying some mathematical algorithms to the values of the pixels in the neighbourhood of the target pixel. In this regard, linear predictive filtering is explained as a common form of filtering in which the output pixel value can be determined as a linear combination of neighbouring pixels magnitudes. Generally, for a typical LPC we derive an algorithm with two separate parts: encoding part and synthesis (decoding) part. In an encoding part, the designed LPC takes the input samples in predefined blocks and determines the input time-series signal and related filter taps in order to reproduce the current block of information. These output data are quantised and passed into the second part. In the decoding section, the filter is reconstructed by LPC based on the received coefficients from the previous part. The whole filter structure can be viewed as a tube that, when is fed by an input signal, produces required information (forecasted values). In predictive coding, different types of filters can be designed and applied to the work, but basically there are two kinds of filters: finite impulse response (FIR) filters and infinite impulse response (IIR) filters. Mostly, the FIR filter function is implemented as a direct form structure as shown in Fig. 4 or (2).

$$\begin{aligned} y(n) = {} & b(1) \times x(n) + b(2) \times x(n-1) \\ & + \cdots + b(nb+1) \times x(n-nb) \\ & - a(2) \times y(n-1) - \cdots - a(na+1) \times y(n-na) \end{aligned} \tag{2}$$

where $n-1$ is the filter order, na is the feedback filter order and nb is the feed forward filter order. In a general manner, the operation of filter at sample is given by the time domain difference equations (3)

$$y(t) = \sum_{\tau=0}^{n-1} h_\tau x(t-\tau), \quad t \in Z$$

$x: Z \to R$ is the input signal; $y: Z \to R$ is the output signal

$h_i \in R$ are called filter coefficients; n is filter order or length (3)

4 Fundamentals of ANN

As mentioned earlier, because ANN has inherent capability for non-linear functionality and accurate mapping, it can be applied for prediction objectives. Furthermore, the stochastic nature of renewable energies makes ANNs powerful tools to overcome limitations accompanied by some conventional linear methods that is, ANNs can be trained wisely to solve any complex problem which is hard to grasp analytically [15]. Generally, the structure of an ANN consists of three basic elements: weights, thresholds and activation function connected by a true learning algorithm. In this regard, back propagation (BP) is a kind of learning algorithm which is both simple and applicable [16]. During BP training phase several algorithms can be applied and a brief description from two of these algorithms is provided here.

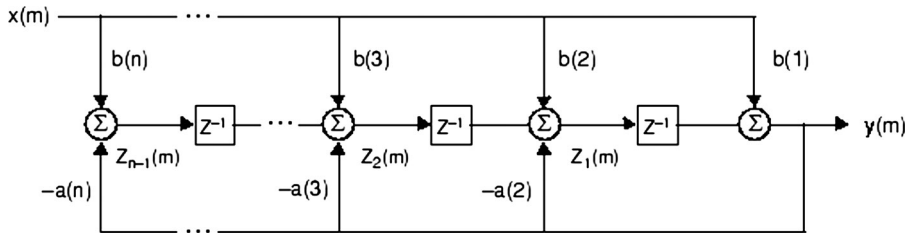

Fig. 4 *Direct form II transposed FIR filter*

4.1 Gradient descent algorithm (basic BP algorithm)

In gradient descent training algorithm the error function, which carries the halved sum of squares of element-wise error terms, is expressed as

$$\varepsilon = \frac{1}{2}\left(\sum_{k=1}^{n}(t_k - o_k)^2\right) \tag{4}$$

where t_k and o_k are the target output and real output, respectively, and k is the number of output data. As said before, network weights and biases must be updated in each epoch and new values are used for subsequent iterations as shown in (5).

Q3

$$\boldsymbol{W}_{ij}(k) = U(k) + m \cdot \boldsymbol{W}_{ij}(k-1) \tag{5}$$

where $\boldsymbol{W}_{ij}(k)$ is the current weights and bias vector, $U(k)$ is the update function and m is the momentum factor which adds a fraction of the previous weights update to the current ones and it is limited between 0 and 1($0 \le m \le 1$). Using gradient descent algorithm the update function ($U(k)$) is calculated as

$$g(k) = \mu\frac{\partial\varepsilon}{\partial W_{ij}(k)} \rightarrow U(k) = -g(k) \tag{6}$$

where μ is the learning rate which controls the step size when weights are iteratively adjusted. It is worthy of note that the basic BP training algorithm works by altering the values of weights with a fixed length vector in the direction of the negative gradient to minimise an error function. In this regard, (4) is valid for the networks that have one output vector.

4.2 Levenberg–Marquardt algorithm

Levenberg–Marquardt (L–M) algorithm is an iterative sequence of instructions similar to any numeric minimisation algorithms and it can find a solution even if the target minimum be far away from the start point [17]. For L–M algorithm the update function $U(k)$ can be computed using (7).

$$U(k) = -[\boldsymbol{J}^{\mathrm{T}} \times \boldsymbol{J} + \beta \times \mathrm{diag}(\boldsymbol{J}^{\mathrm{T}} \times \boldsymbol{J})]^{-1} \times \boldsymbol{J}^{\mathrm{T}} \times \boldsymbol{\varepsilon} \tag{7}$$

where $\boldsymbol{J}$ is the Jacobian matrix which includes first-order derivatives of the network errors with respect to the weights and biases, and $\boldsymbol{\varepsilon}$ is the vector of network errors. β is a non-negative scalar number called damping factor and diag is an abbreviation for diagonal matrix which is equal to identity matrix in this equation.

5 Designing linear predictive digital FIR filters

In linear forecasting, future samples or target outputs can be optimally estimated through an autoregressive process using a linear combination of past samples. Suppose that the present values of the climatic data are predicted by the past M samples of the related signal such that

$$\begin{aligned}\tilde{x}(n) &= a_1 x(n-1) + a_2 x(n-2) + \cdots + a_M x(n-M) \\ &= \sum_{i=1}^{M} a_i x(n-i)\end{aligned} \tag{8}$$

where $\tilde{x}(n)$ is the estimation of $x(n)$, $x(n-i)$ is the ith step previous sample, and $\{a_i\}$ is regarded as the vector of linear prediction coefficients. The error between the real value and the estimated one can be expressed as

$$\varepsilon(n) = x(n) - \tilde{x}(n) = x_n - \sum_{i=1}^{M} a_i x(n-i) \tag{9}$$

To find optimal filter coefficients that best describe the current plan of action, first the error function must be minimised in the sense of mean squared error (10).

$$E = \sum_n \varepsilon^2(n) = \sum_n (x(n) - \sum_{i=1}^{M} a_i x(n-i))^2 \tag{10}$$

The most accurate tap vector $\{a_i\}$ can be found by minimising the sum of the squared error. If the first-order derivative of E with respect to a_i set to zero (using the chain rule), one obtains

$$\begin{aligned}&2\sum_n x(n-k)\left(x(n) - \sum_{i=1}^{M} a_i x(n-i)\right) = 0 \\ &\quad \text{for } k = 1, 2, 3, \ldots, M\end{aligned} \tag{11}$$

Taking the above derivatives yields M equations that can be written as

$$\begin{aligned}&a_1 \sum_n x(n-k)x(n-1) + a_2 \sum_n x(n-k)x(n-2) \\ &\quad + \cdots + a_M \sum_n x(n-k)x(n-M) \\ &\quad = \sum_n x(n-k)x(n); \quad \text{for } k = 1, 2, 3, \ldots, M\end{aligned} \tag{12}$$

Suppose that an input signal is divided into several frames each with N samples. If each frame length is short enough

doi: 10.1049/iet-rpg.2010.0104

then the signal in the related frame may be stationary. It should be also noted that the signal equals zero out of the current template range. If N samples exist in the sequence categorised from 0 to $N-1$, $\{x_n\} = \{x(0), x(1), x(2), \ldots, x(N-2), x(N-1)\}$ then (12) can be stated in terms of a matrix equation as given in (13)

$$\begin{bmatrix} r(0) & r(1) & r(2) & \cdots & r(M-2) & r(M-1) \\ r(1) & r(0) & r(1) & \cdots & r(M-3) & r(M-2) \\ r(2) & r(1) & r(0) & \cdots & r(M-4) & r(M-3) \\ \vdots & \vdots & \vdots & & \vdots & \vdots \\ \vdots & \vdots & \vdots & & \vdots & \vdots \\ r(M-1) & r(M-2) & r(M-3) & \cdots & r(1) & r(0) \end{bmatrix} \times \begin{bmatrix} a_1 \\ a_2 \\ a_3 \\ \vdots \\ a_{M-1} \\ a_M \end{bmatrix} = \begin{bmatrix} r(1) \\ r(2) \\ r(3) \\ \vdots \\ r(M-1) \\ r(M) \end{bmatrix}$$

$$R \cdot a = r \tag{13}$$

where

$$r(k) = \sum_{n=0}^{N-1-k} x(n)x(n+k) \tag{14}$$

The above calculation is generally called the autocorrelation method [18] and if such a method is applied for designing

Table 1 Correlation coefficients between solar radiation data within the template

$\rho_{i,j}$	$j=0$	$j=1$	$j=2$	$j=3$
$i=0$	1	0.94738	0.83410	0.68275
$i=1$	0.83428	0.80376	0.71825	0.59514
$i=2$	0.81116	0.80191	0.69842	0.57903
$i=3$	0.83259	0.79878	0.71644	0.59287

Table 2 Correlation coefficients between wind speed data within the template

$\rho_{i,j}$	$j=0$	$j=1$	$j=2$	$j=3$
$i=0$	1	0.97679	0.93389	0.87019
$i=1$	0.87403	0.87051	0.86210	0.84807
$i=2$	0.87410	0.86995	0.86103	0.83261
$i=3$	0.86651	0.86178	0.84759	0.84582

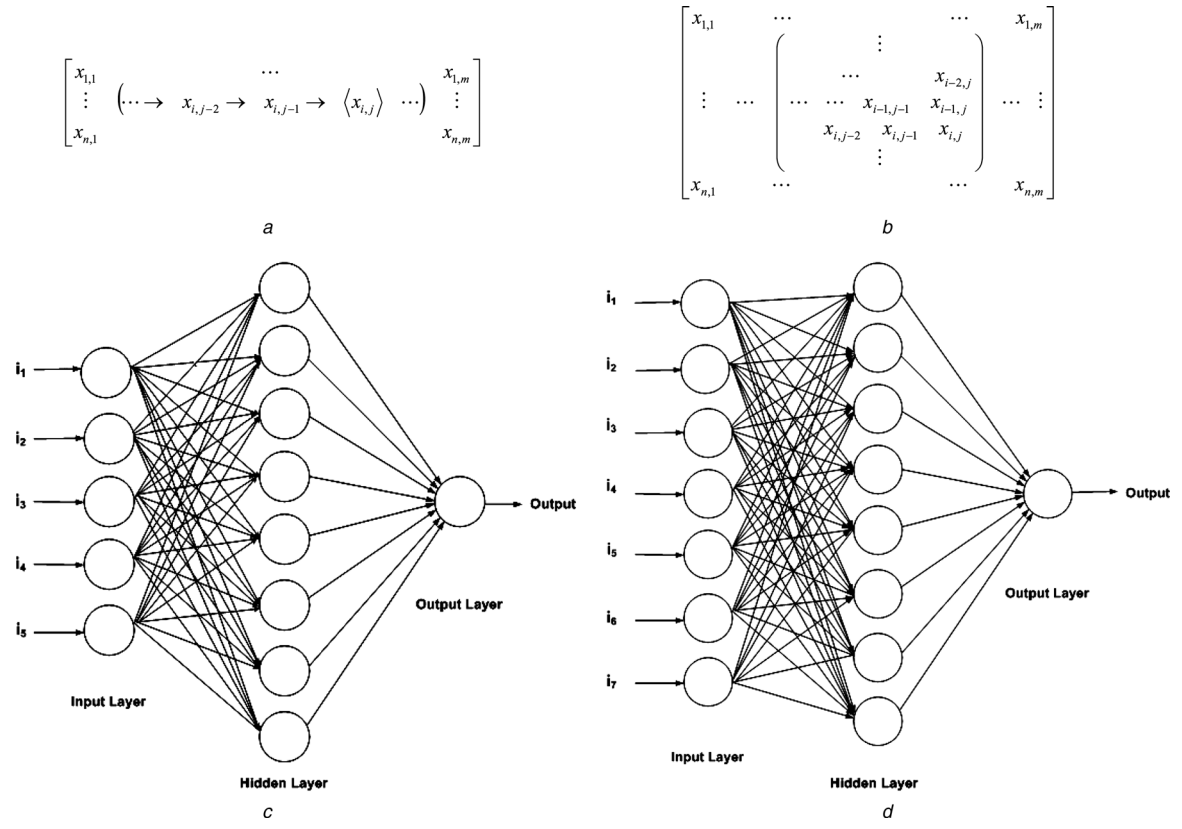

Fig. 5 *Different types of prediction models*

a 1-D horizontal prediction
b 2-D FIR filter
c Equivalent NN of a fifth-order FIR filter (NN/5th)
d Equivalent NN of a seventh-order FIR filter (NN/7th)

process the synthesis filter will be stable. To solve the matrix equation and calculate the filter coefficients first it is needed to compute the inverse of correlation matrix (R^{-1}). Since R is a symmetric matrix with similar diagonal elements, the inversion action can be done easily using some recursive approaches like Levinson–Durbin (L–D), which is computationally efficient while determining the filter coefficients using (15)

$$a = R^{-1} r \tag{15}$$

It should be mentioned that for a time-varying series the correlation coefficient (ρ) between two random variables with expected values μ_x and μ_Y and standard deviations σ_X and σ_Y is defined as

$$\rho_{X,Y} = \mathrm{Corr}(X, Y) = \frac{\mathrm{cov}(X, Y)}{\sigma_X \sigma_Y} = \frac{E[(X - \mu_X)(Y - \mu_Y)]}{\sigma_X \sigma_Y} \tag{16}$$

where E is the mathematical expectation, cov(X, Y) means covariance between X and Y variables and Corr is a famous notation for Pearson's correlation [18].

5.1 2-D FIR filters against 1-D representations and ANNs

To evaluate the performance of the purposed filters different types of structures are designed and tested via similar data. First a horizontal model is created and treated as an example for conventional 1-D prediction. Then three types of 2-D FIR filters are constructed and considered as the proposed estimation approach in this paper and finally two NNs are designed as non-linear predictive models with similar input pattern to those of 2-D models. The accuracy of the models is compared in terms of maximum prediction error, root mean square error (RMSE) and the correlation between predicted and actual data ($\rho_{\mathrm{est-act}}$).

It must be pointed out that in LPC it is proved that a precise and robust 2-D forecasting process relies on applying highly correlated information [19]. The more the correlated data results, the less the prediction error and the more the forecasting quality. In this regard, correlation coefficients between solar radiation and wind speed data within a template with four pixels in length and width, showing four

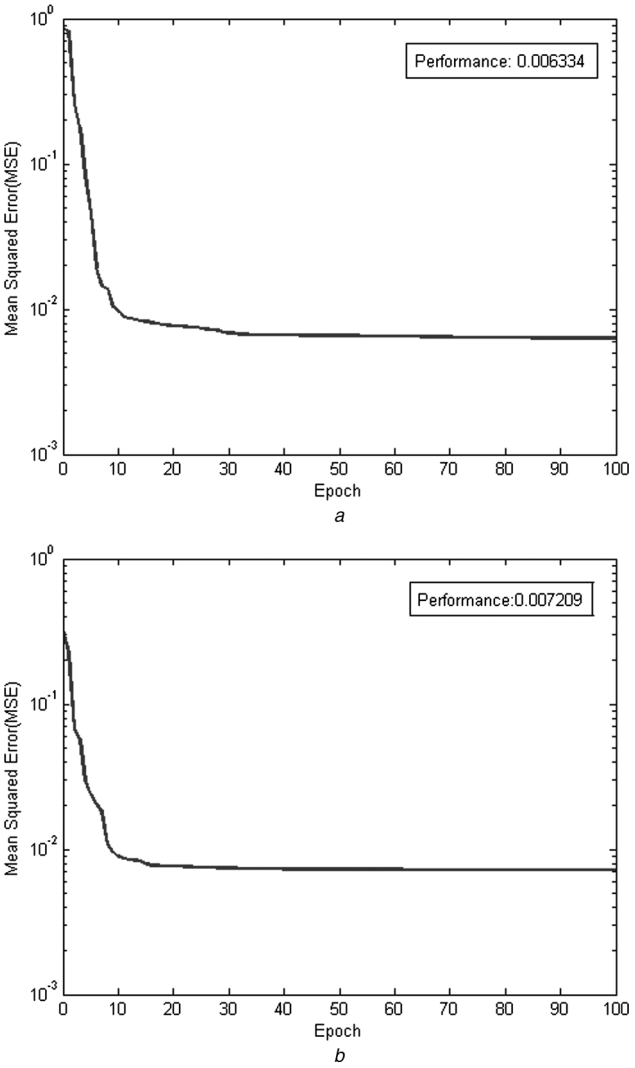

Fig. 6 *Performance curve of 5th-NN as a function of epoch numbers*

a Solar radiation prediction performance
b Wind speed prediction performance

Table 3 Optimal filter taps weights for solar radiation prediction

Filter type	h_1	h_2	h_3	h_4	h_5	h_6	h_7
1-D type 1 (horizontal FIR filter)	1.398087	− 0.31506	− 0.17252	N/A*	N/A	N/A	N/A
2-D type 1 (3rd-order FIR filter)	1.434167	− 0.37205	− 0.16102	N/A	N/A	N/A	N/A
2-D type 2 (5th-order FIR filter)	1.296368	1.296368	0.080054	0.03978	0.078725	N/A	N/A
2-D type 3 (7th-order FIR filter)	1.274913	− 0.52869	0.05721	0.022567	0.058618	0.043944	0.035129

N/A: not available.

Table 4 Optimal filter taps weights for wind speed prediction

Filter type	h_1	h_2	h_3	h_4	h_5	h_6	h_7
1-D type 1 (horizontal FIR filter)	0.377694	0.209899	0.361598	N/A*	N/A	N/A	N/A
2-D type 1 (3rd-order FIR filter)	0.8716971	0.159227	−0.05037	N/A	N/A	N/A	N/A
2-D type 2 (5th-order FIR filter)	0.893364	0.206905	−0.08787	0.021717	−0.06018	N/A	N/A
2-D type 3 (7th-order FIR filter)	0.08103	0.019701	0.048049	0.811706	0.144028	−0.07116	−0.03866

N/A: not available

doi: 10.1049/iet-rpg.2010.0104

consecutive hours a day and four consecutive days in a year are tabulated in Tables 1 and 2 using (16).

Conventional forecasting methods are generally based on utilising past samples in a 1-D template that refers to a horizontal prediction as shown in Fig. 5*a*. Such a method can be found in [20], applying 14, 15, 28 and 29 weather samples before the hour to be forecasted. It is observed from the first rows of Tables 1 and 2 that horizontal pixels are highly correlated and they can act properly in forecasting process. Now, the plan of action changes from formal 1-D approaches to expert 2-D one which takes advantages from highly correlated information in both directions within the template domain. Referring to Tables 1 and 2, again it is observed that correlation coefficients between meteorological data decrease as long as i and j increase across the template and the neighbouring pixels in multiple directions which convey information from previous hours and days contain strong correlations with

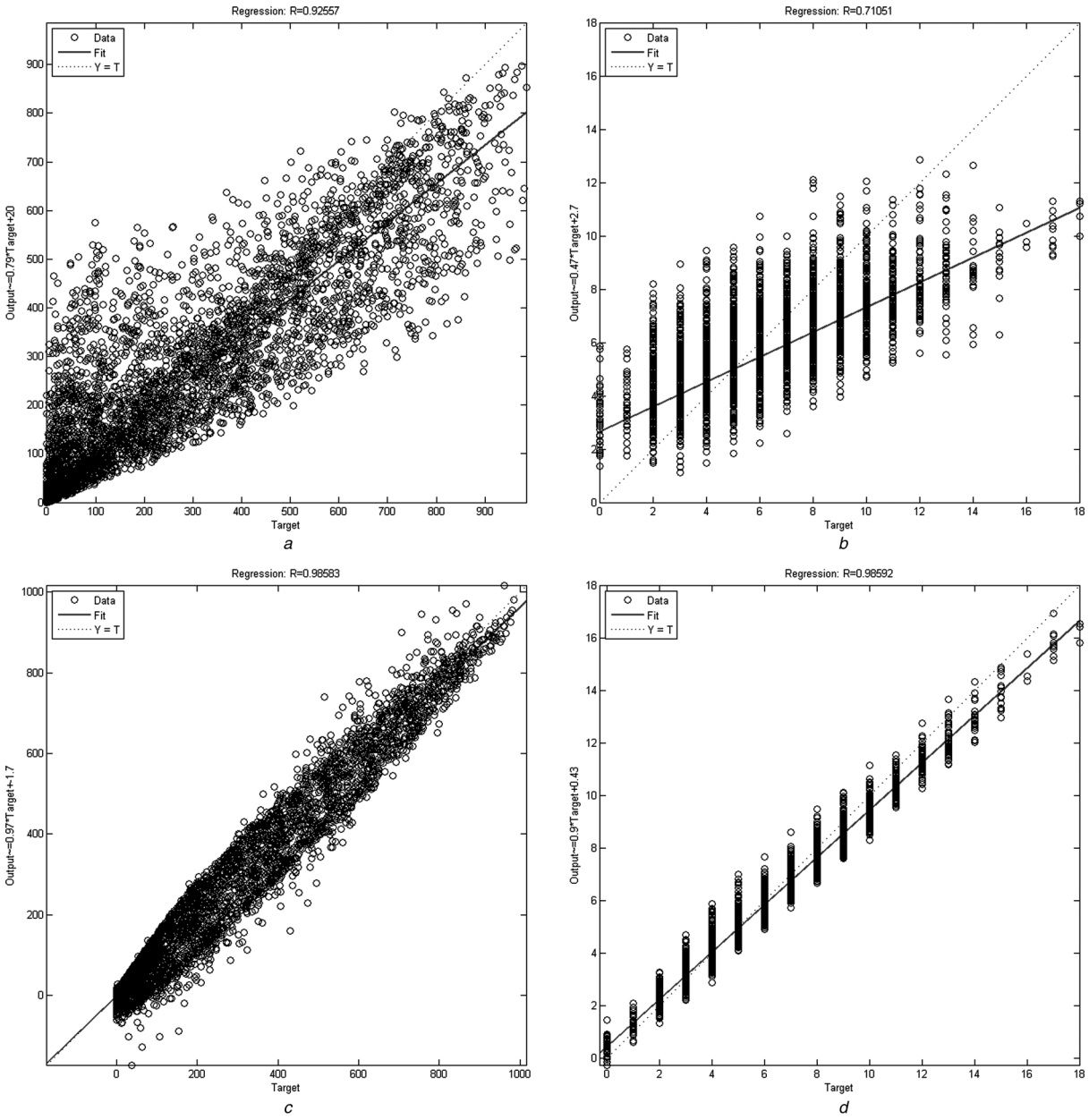

Fig. 7 *Performances of different models in the case of solar radiation and wind speed forecasting*

a Solar radiation
b Wind speed: 1-D horizontal forecasting performance
c Solar radiation
d Wind speed: 2-D forecasting performance (third-order FIR filter)
e Solar radiation
f Wind speed: 2-D forecasting performance (fifth-order FIR filter)
g Solar radiation
h Wind speed: 2-D forecasting performance (seventh-order FIR filter)
i Solar radiation
j Wind speed: NN/5th forecasting performance
k Solar radiation
l Wind speed: NN/7th forecasting performance

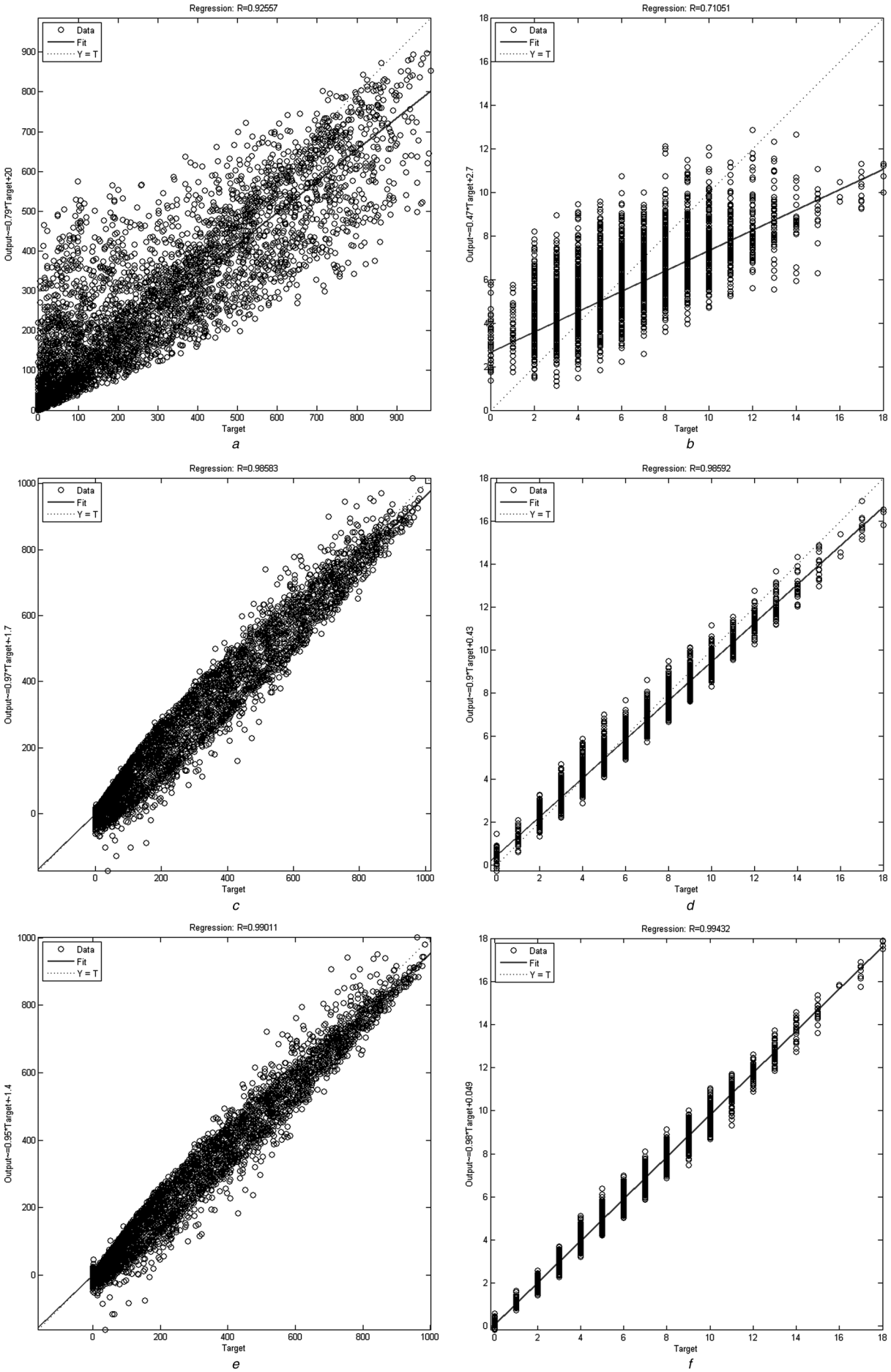

Fig. 7 *Continued*

doi: 10.1049/iet-rpg.2010.0104

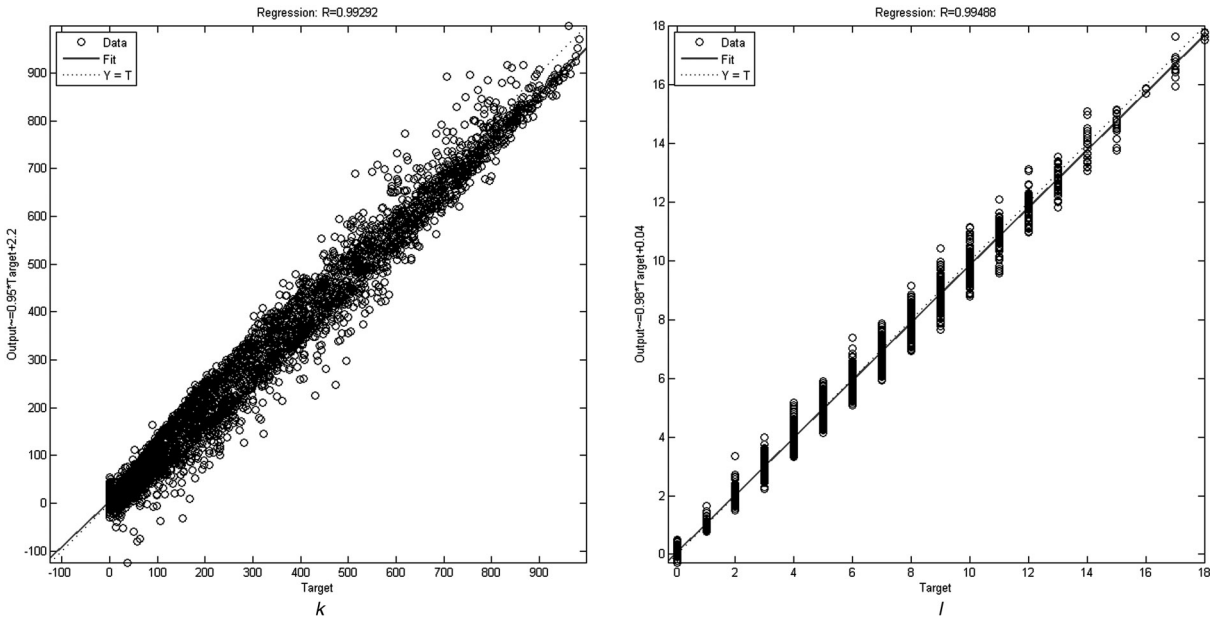

Fig. 7 *Continued*

each other. Therefore considering a set of pixels with the highest correlations can be a decisive factor for implementation of expert 2-D FIR filters as shown in Fig. 5*b*. Here, to assess the 2-D forecasting performance by means of non-linear functions two NN architectures are adopted and fed by similar data. Each NN is constructed on the basis of its equivalent 2-D FIR filter mentioned above and has multiple inputs chosen from the template domain, similar to those of 2-D models, and a single output relates to estimated value as shown in Figs. 5*c* and *d*. In this regard, since the input data values and their patterns are the same in the NNs architectures and the proposed 2-D FIR filters, the comparison of results are possible and valid. Solar radiation and wind speed data from 10 months of the typical year are selected randomly for training phase and the rest are used for testing process. For both networks S-shaped (sigmoidal) activation function is utilised and the previously mentioned learning algorithms (gradient descent, L–M) are applied for training phase. The number of neurons in hidden layer is also determined experimentally through a trial and error action.

5.2 Forecasting performance evaluation

In order to assess the performance of purposed FIR filters the exact template size and optimal filter coefficients must be computed so as to fit the needs. Tables 3 and 4 indicate optimal tap weights of different 1-D and 2-D filters for solar radiation and wind speed prediction using (15).

To derive the equivalent NN architectures, first the number of inputs must meet the requirements. Since we want to compare the performances in the case of linear and non-linear prediction the input vector must be the same in both structures. For example if a FIR filter uses five input pixels with the highest correlations, known as fifth-order FIR filter, then the same input data from the same positions inside the 2-D template are selected for the equivalent NN of that FIR filter (NN/5th).

For better convergence of NNs solar radiation and wind speed data are normalised between -1 and $+1$ linearly. Moreover, from various training algorithms two are selected and compared in terms of prediction error and resemblance of predicted values to target values. It is observed that L–M algorithm shows better performance, therefore it is applied for training phase of both networks. It is found experimentally that using eight neurons in the hidden layer together with L–M training algorithm provides the best performance and the least prediction error. As an example, Figs. 6*a* and *b* show the performance curve for NN/5th as a function of epochs in the case of solar radiation and wind speed prediction. It is observed from Fig. 6 that during learning phase the desired performance is obtained within 30 and 15 epochs for solar radiation and wind speed forecasting, respectively, although the learning algorithm is run 100 epochs for each prediction model.

The performance evaluation of models begins with the horizontal prediction. A set of data including three samples from previous hours in a same day feeds the prediction model and forecasted values are obtained, respectively, as shown in Figs. 7*a* and *b*. The second model known as third-order FIR filters again applies three samples with the highest correlation but from previous hours and days considering a 2-D template domain. As shown in Figs. 7*c* and *d* the forecasting performance improves greatly in comparison with that of horizontal one, although the number of input data remains unchanged. In this regard, if we extend the 2-D filtering window (up to a limit range) and use more samples from both directions the performance shows further improvement as shown in Figs. 7*e–h*. Finally, to assess the prediction performance by means of non-linear forecasting two NNs are designed and trained on the basis of their equivalent 2-D representations regarding the previously mentioned focal points. Figs. 7*i–l* indicate the performances of NN/5th and NN/7th in the case of solar radiation and wind speed forecasting, respectively. It is observed from simulation results, although the performances of NN-based approaches outweigh the ones from 2-D FIR predictive filters in low orders (e.g. 5th-order) but different results are achieved in higher orders and better performance from the proposed method is observed.

Table 5 Performance assessment of predictors in solar radiation forecasting

Predictor type	Max. error, W/m^2	RMSE	$\rho_{\text{est-act}}$
1-D type 1 (horizontal FIR filter)	425.32	64.373	0.95878
2-D type 1 (3rd-order FIR filter)	269.96	38.823	0.98583
2-D type 2 (5th-order FIR filter)	247.38	36.345	0.99011
2-D type 3 (7th-order FIR filter)	200.61	22.726	0.99537
NN type 1 (NN equivalent of 5th-order FIR filter-NN/5th)	246.72	33.011	0.99048
NN type 2 (NN equivalent of 7th-order FIR filter-NN/7th)	224.45	29.896	0.99292

Table 6 Performance assessment of predictors in wind speed forecasting

Predictor type	Max. error, m/s	RMSE	$\rho_{\text{est-act}}$
1-D type 1 (horizontal FIR filter)	2.6114	0.599	0.97429
2-D type 1 (3rd-order FIR filter)	2.4317	0.573	0.98592
2-D type 2 (5th-order FIR filter)	2.1763	0.277	0.99432
2-D type 3 (7th-order FIR filter)	1.4118	0.251	0.99523
NN type 1 (NN equivalent of 5th-order FIR filter-NN/5th)	2.2829	0.287	0.99416
NN type 2 (NN equivalent of 7th-order FIR filter-NN/7th)	1.5707	0.257	0.99488

6 Results and discussions

Experimental observations indicate that image processing tools and predictive filtering can be powerful means to overcome the stochastic nature of renewable energies and enhance the prediction of their behaviours to a great extent. According to the 2-D image-like model it is observed that adjacent pixels in a given template are more correlated than the others in farther distances, therefore using predictive filtering based on strong correlation values can improve the forecasting capability. Furthermore, it is indicated that meteorological data such as solar radiation and wind speed at consecutive hours a day (pixels in horizontal positions) carry high correlations similar to climatic data at a given hour among consecutive days (pixels in vertical positions), although correlation values among the latter group are lower compared to the former. As a rule, considering a 2-D template with a set of highly correlated pixels can be the best respondent to the forecasting needs.

To summarise the performance of all prediction models that had been put forth, RMSE and the maximum likelihood of predicted values against the actual ones ($\rho_{\text{est-act}}$) are calculated and tabulated as given in Tables 5 and 6.

According to Tables 5 and 6, the RMSE values achieved for 2-D models are obviously smaller than the values obtained from 1-D ones, although these values may become slightly bigger in comparison with values from some kinds of NN structures. As a whole, the 2-D predictors' performances outweigh the resultant performances from both 1-D modelling and NN-based approaches. Furthermore, the results indicate that applying larger 2-D templates up to a limit range together with optimal filter sizing ends in higher performance and more trustful forecasting.

7 Conclusions

So far, many various models for predicting renewable energies have been purposed and mostly are based on physical methods or conventional statistical ones. Some others apply ANN techniques or combined methods such neuro-fuzzy algorithms or wavelet transformations. Anyway, forecasting methods are generally based on 1-D routine algorithm and few of them purposed 2-D modelling such as [14], but a lack of accuracy can be found in all of them. On the other side, with high levels of renewable energy penetration in smart grids the overall effect on grid operations will increase consequently; therefore, there is a strong need to forecast maximum power generation from these resources accurately. In this work, various types of 1-D and 2-D FIR filters along with some NN architectures are designed for solar radiation and wind speed forecasting and their performances are evaluated using similar data. It is indicated that an intelligent 2-D structure gives a better forecasting both in the case of RMSE and maximum likelihood ($\rho_{\text{est-act}}$), compared to 1-D conventional types or their equivalent NN-based models. Moreover, it is observed from simulation results that in the case of 2-D filtering, prediction results are closely matching actual data along the diagonal axis, the slope of the linear fit is close to 45° and the scatter is narrow along the matching diagonal axis, which indicates a successful prediction with high correlation and small deviation correspondingly.

8 References

1 Hammons, T.J.: 'Integrating renewable energy sources into European grids'. Proc. 41st Int. Universities Power Engineering Conf., 2006 (UPEC '06), 2006, vol. 1, pp. 142–151

2 Helander, A., Holttinen, H., Paatero, J.: 'Impact of wind power on the power system imbalances in Finland', *IET Renew. Power Gener.*, 2010, **4**, (1), pp. 75–84

3 Boehme, T., Harrison, G.P., Wallace, A.R.: 'Assessment of distribution network limits for non-firm connection of renewable generation', *IET Renew. Power Gener.*, 2010, **4**, (1), pp. 64–74

4 Ummels, B.C., Pelgrum, E., Gibescu, M., Kling, W.L.: 'Comparison of integration solutions for wind power in the Netherlands', *IET Renew. Power Gener.*, 2009, **3**, (3), pp. 279–292

5 Muneer, T., Gul, M.S.: 'Evaluation of sunshine and cloud cover based models for generating solar radiation data', *Energy Convers. Manag.*, 2000, **41**, (5), pp. 461–482

6 Muneer, T., Gul, M.S., Kubie, J.: 'Models for estimating solar radiation and illuminance from meteorological parameters', *J. Solar Energy Eng. Trans. ASME*, 2000, **122**, (3), pp. 146–153

7 Tobiska, W.K.: 'Status of the SOLAR2000 solar irradiance model', *Phys. Chem. Earth, Part C: Solar Terres. Planet Sci.*, 2000, **25**, (5), pp. 383–386

doi: 10.1049/iet-rpg.2010.0104

8 Reddy, K.S., Manish, R.: 'Solar resource estimation using artificial neural networks and comparison with other correlation models', *Energy Convers. Manage.*, 2003, **44**, pp. 2519–2530

9 Giebel, G., Landberg, L., Kariniotakis, G., Brownsword, R.: 'State-of-the-art on methods and software tools for short-term prediction of wind energy production'. Proc. EWEC, Madrid, Spain, 2003

10 Landberg, L., Giebel, G., Nielsen, H.A., Nielsen, T., Madsen, H.: 'Short-term prediction – an overview', *Wind Energy (Special Review Issue on Advances in Wind Energy)*, 2003, **6**, (3), pp. 273–280

11 Barbounis, T.G., Theocharis, J.B., Alexiadis, M.C., Dokopoulos, P.S.: 'Long-term wind speed and power forecasting using local recurrent neural network models', *IEEE Trans. Energy Convers.*, 2006, **21**, (1), pp. 273–284

12 Chaabene, M., Ben Ammar, M.: 'Neuro-fuzzy dynamic model with Kalman filter to forecast irradiance and temperature for solar energy systems', *Renew. Energy*, 2008, pp. 1435–1443 **Q5**

13 Cao, J.C., Cao, S.H.: 'Study of forecasting solar irradiance using neural networks with preprocessing sample data by wavelet analysis', *Energy*, 2006, **3**, pp. 13435–13445

14 Hocaoğlu, F.O., Gerek, Ö.N., Kurban, M.: 'A novel 2-D model approach for the prediction of hourly solar radiation', (*LNCS* **4507**), (Springer, 2007), pp. 741–749

15 Fausset, L.: 'Fundamentals of neural networks' (Prentice-Hall, Upper Saddle River, NJ, 1994)

16 Haykin, S.: 'Neural networks: a comprehensive foundation' (Prentice-Hall, Upper Saddle River, NJ, 1999)

17 Levenberg, K.: 'A method for the solution of certain non-linear problems in least squares', *Quart. Appl. Math.*, 1944, **2**, pp. 164–168

18 Rodgers, J.L., Nicewander, W.A.: 'Thirteen ways to look at the correlation coefficient', *Am. Statist.*, 1988, **42**, pp. 59–66 [doi:10.2307/2685263]

19 Gonzalez, R.C., Woods, R.E.: 'Digital image processing' (Prentice-Hall, Englewood Cliffs, USA, 2002, 2nd edn.), pp. 461–463

20 Cao, J., Lin, X.: 'Study of hourly and daily solar irradiation forecast using diagonal recurrent wavelet neural networks', *Energy Convers. Manage.*, 2008, **49**, (6), pp. 1396–1406

21 Intersil^{TM}. 'An introduction to digital filters. Application note', 1999, AN9603.2. www.intersil.com **Q6**

22 Douglas, S.C.: 'Introduction to adaptive filters'. Digital signal processing handbook 1999, pp. 7–12 **Q7**

23 Nelson, M., Gailly, J.-L.: 'Speech compression'. The data compression book 1995, pp. 289–319 **Q7**

24 Dukpa, A., Duggal, I., Venkatesh, B., Chang, L.: 'Optimal participation and risk mitigation of wind generators in an electricity market', *IET Renew. Power Gener.*, 2010, **4**, (2), pp. 165–175

www.ietdl.org

RPG20100104

Author Queries

A. Anvari Moghaddam, A.R. Seifi

Q1 References are renumbered to get the sequence order. Please check

Q2 Please check the sentence "Moreover, since the 2-D modeling… information for operators." for sense clarity

Q3 IET style for matrices and vectors is to use bold italics. Please check that we have identified all instances correctly

Q4 Please provide the significant of asterik (∗) in table body of Tables 3 and 4

Q5 Please provide volume number for Ref. 12

Q6 Refs. 21-24 are not cited in the text. Please cite in the text, else delete from the list

Q7 Please provide publisher name in Ref. [22,23]